Cement and Concrete Research 40 (2010) 1495–1506

Contents lists available at ScienceDirect

Cement and Concrete Research

journal homepage: http://ees.elsevier.com/CEMCON/default.asp

Controlled telescopic reinforcement system of fabric–cement composites — Durability concerns

Zvi Cohen [a], Alva Peled [b,*]

[a] Department of Materials Engineering, Ben-Gurion University of the Negev, Beer-Sheva, Israel
[b] Department of Structural Engineering, Ben-Gurion University of the Negev, Beer-Sheva, Israel

ARTICLE INFO

Article history:
Received 7 April 2009
Accepted 4 June 2010

Keywords:
Interfacial transition zone (B)
Long-term performance (C)
Mechanical properties (C)
Fillers (D)
Textile reinforcement

ABSTRACT

The study objective was to modify the microstructure of AR glass strand to induce a controlled mode of telescopic bonding during service life, by using sub-micron particles absorbed between the filaments of the strand. Two groups of fillers were used: (i) pozzolanic fillers (silica fume) with 50 nm and 200 nm particle sizes; and (ii) polymeric fillers (polystyrene-based polymers), with two glass transition temperatures (−6 °C and 100 °C). Composites were prepared using fabric reinforcement and tested for tensile behavior. Composite properties could be controlled by addition of fillers into the glass bundle, and the magnitude and efficiency of the modification was highly dependent on the filler type, structure, and properties. The best performance was obtained with silica fume fillers having relatively large 200 nm particles.

1. Introduction

In recent years there has been considerable interest in FRC (fiber/fabric reinforced cement/concrete) and ways to improve their mechanical performance [1]. Addition of fibers/fabrics as reinforcement for the brittle cement matrix can greatly improve its tensile strength, elongation to failure, and energy consumption [2–6]. Most high performance fibers are in the form of multifilament bundles (roving) with a wide range of fiber properties and can be assembled into technical fabrics, which can be tailored for high performance cementitious composites with controlled two- and three-dimensional geometry.

The use of man-made multifilament reinforcement for cementitious materials has numerous advantages. However, the cement matrix consists of relatively large particles (~10 μm) that are larger than the spaces between the filaments of the strand; therefore, the cement particles cannot fully penetrate the inter-bundle spacing. This results in unique bonding mechanisms, whereby the external filaments ("sleeve") are in intimate contact with the hydration products and the internal filaments ("core") are relatively free [4,6–8]. Due to this special microstructure of the reinforcing bundle, the external filaments (sleeve filaments), which are in direct contact with the cement matrix and well bonded to the matrix, are fractured during loading, providing high first crack stress. After their failure a telescopic type of pullout is generated, whereby the internal filaments ("core" filaments) slip against the external ("sleeve") filaments (Fig. 1). This sliding mode of the inner filaments induces high ductility to the composite, mostly when brittle fibers are used. The telescopic mode of failure has been described in particular for glass strands [6–8], and can be considered a favorable effect for glass fiber-reinforced cement composite (GFRC) systems.

During continued hydration and aging a slow and gradual process of deposition of hydration products between the filaments takes place, which may change the nature of bonding by increasing the sleeve/core ratio. This results in a stronger bond, which is a favorable effect but may also lead to embrittlement, mainly when brittle fibers such as glass are used [6,8,9]. This means that the bonding changes over time and thus also the composite properties and durability. Another change of GFRC over time is caused by chemical attack of the glass fibers when they are surrounded by cement hydrates [10]. The diffusion process of the cement products over time, between the filaments of the bundle, can lead to intensive corrosion of the glass filaments, since more fibers are in direct contact with the hydrate products of the cement paste matrix, the reduction of the overall behavior, toughness, and strength of the GFRC is more severe.

To get high composite performance, there is a need to ensure efficient composite action by transfer the forces from the matrix to the bundle filaments. Stress transfer between those two components is dependent on the bond developed between them; as the bond increases, the transfer of stresses will improve. In the case of multifilament reinforcements, the bonding and stress transfer between the external filaments and the matrix are better than that of the inner filaments and the matrix.

Based on the above, when dealing with multifilament reinforcements and cement matrices three main approaches should be considered concurrently: (i) improving the stress transfer between the inner filaments and the cement matrix, in order to improve

* Corresponding author. Tel.: +972 8 6479672; fax: +972 9 6479670.
E-mail address: alvpeled@bgu.ac.il (A. Peled).

0008-8846/$ – see front matter © 2010 Elsevier Ltd. All rights reserved.
doi:10.1016/j.cemconres.2010.06.003

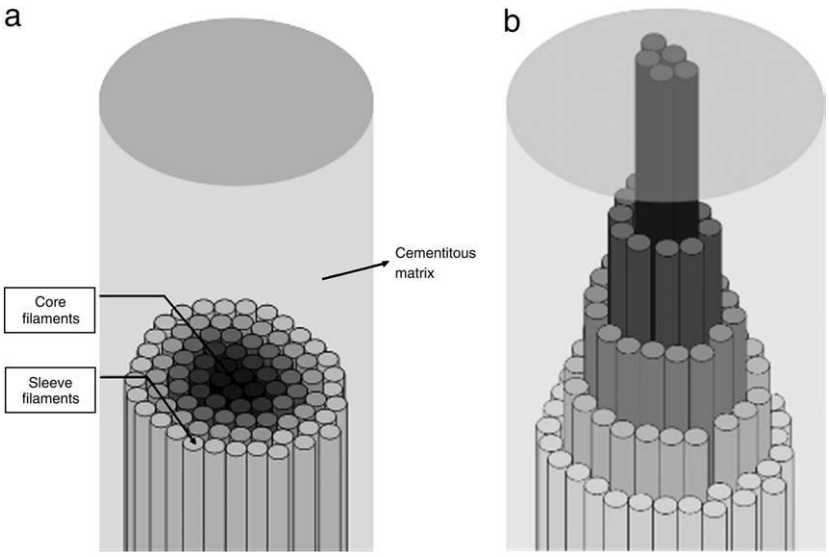

Fig. 1. (a) The core and sleeve zones in the bundle before pullout, (b) the telescopic pullout behavior (after the pullout process).

bonding and the overall performance of the composite; (ii) limiting the deposition of the hydration products between the filaments of the strand during aging, to keep the telescopic mode of failure and the related composite ductile behavior, mainly with brittle fibers; and (iii) lowering matrix penetrability between the bundle filaments, in order to reduce corrosion effects when glass fibers are used, as fewer fibers are in direct contact with the cement paste products.

The objective of the current study was to modify the microstructure of AR glass strands surface to induce a controlled mode of telescopic bonding: (i) to achieve maximum first crack stress and ductility; (ii) to keep the telescopic mode constant through the whole service life of the composite, so it will not be affected by the continued hydration of the surrounding matrix; and (iii) to ensure an efficient stress transfer between the filaments and matrix, to guarantee good composite action. These goals were achieved by using sub-micron organic and inorganic particles, which were tailored to provide a frictional/adhesion phase. AR glass strands in fabric form were used for this study. Tensile tests were performed and the stress–strain responses as well as the change in crack spacing during testing were recorded and correlated with microstructural features. Specimens after accelerated aging were tested and compared. For the un-aged specimens pullout tests were also performed to evaluate the bond strength of each filler system. Composites without fillers made with "clean" fabrics were also tested for comparison.

2. Experimental

2.1. Matrix and reinforcement

The matrix of the composite was plain cement (only cement and water) with 0.4 W/C ratio, using cement type CEM II 42.5 N/B-LL. The paste was mixed for 10 min before applying it to the textile fabrics. The plain matrix properties (without fabric) were tested by split test and its indirect tensile strength was calculated by Eq. (1).

$$\sigma = \frac{f}{\pi}\frac{2F}{ah} \tag{1}$$

where: f — geometry factor due to the shape of the beam and the machine calibration ($f = \sqrt{3}$), F — applied force [N], a — beam width perpendicular to the force axis (70 mm), h — beam height parallel to the force axis (70 mm).

The reinforcement material for this research was warp knitted fabric with an open structure (Fig. 2), to allow cement penetrability between the fabric openings. In these knitted fabrics, straight yarns in the warp direction (lengthwise) were assembled together with straight yarns in the weft direction (crosswise) by stitches (loops). In the warp direction the yarns were arranged in a "two in–two out" formation, in such a manner that there are two yarns close together (as a pair) and then a gap with the size of two yarn diameters separating each pair of yarns. In the weft direction each yarn was separated by a single gap from its neighbor yarn (Fig. 2). All yarns, warp and weft, were in a multifilament form, non-twisted, made from AR glass fibers (Cem-FIL© grade). Two fabrics were tested, differing in the tex size of their warp bundles, 1200 tex and 2400 tex (tex is the weight of a 1000-meter bundle). The 2400 tex bundle, with a diameter of 1.07 mm, is thicker than the 1200 tex bundle, with a diameter of 0.76 mm. Also, these bundles differ in the diameter of their single filaments, 24 μm and 17 μm for the 2400 tex and 1200 tex bundles, respectively. Both fabrics had 1200 tex weft bundles attached to the warp bundles with 16.7 tex PP tricot stitches. Both fabrics were tested for their tensile properties in the warp and weft directions.

2.2. Fillers

In order to achieve a stable and controlled telescopic bonding mechanism, two groups of sub-micron fillers were examined: inorganic silica fume-based particles and inert polymeric particles (200 nm or smaller). For the silica fume, two sizes of particles were used, and for the polymeric fillers two polystyrene polymers having different glass temperatures (T_g) were used. The fillers were in the form of a slurry; four slurries, each consisting of about 50% solid content of inorganic and polymeric materials were used: (i) SFL — Silica Fume with large particles of 200 nm (ii) SFS — Amorphous Silica with small particles of 50 nm, (iii) PSP — Polystyrene polymer which is not film-forming (T_g is higher than room temperature, 100 °C), and (iv) SAF — Styrene Acrylic polymer, which is film-forming (T_g is lower than room temperature, −6 °C). Detailed properties and features of the fillers are shown in Table 1.

The fillers were applied to the fabric bundles by immersing the reinforcement in the slurry for several seconds using the pultrusion process to push the fillers into the bundle. After treatment, the reinforcement was dried for 24 h in laboratory conditions (60% RH,

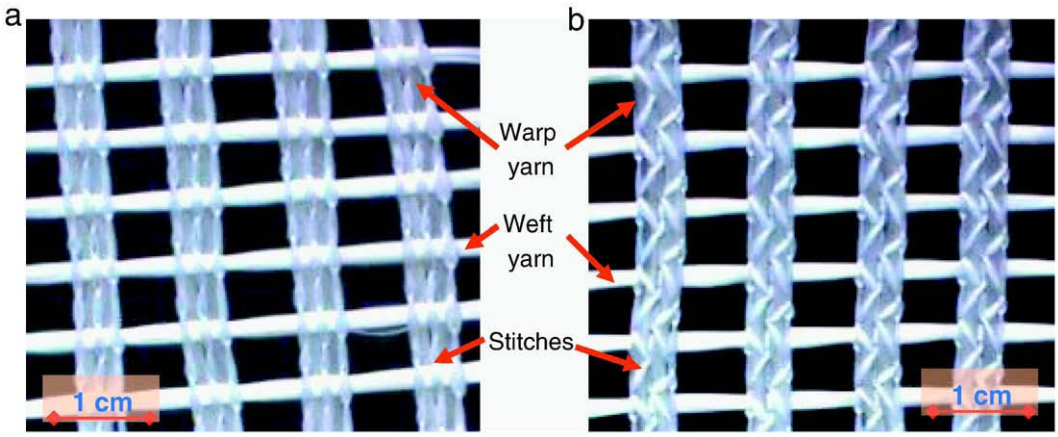

Fig. 2. Both sides of the AR glass knitted fabric used for this research.

23 °C). The dry impregnated fabric was then used to prepare the laminated composites for the tensile tests as described below.

2.3. Specimen preparation

Fabrication of the composite material was done by the pultrusion method (Fig. 3). This method can induce cement matrix penetration into the fabric opening and the filaments of the bundles, by squeezing the cement particles into the fabric [3,11]. Pultrusion was used first to embed the fabric with the different fillers to create a semi-composite fabric as described above; then, in a second step, the filler-treated fabrics were impregnated in a paste of 0.4 water/cement ratio, to produce the laminated specimens. In all the composites with the fillers, the warp yarns of the fabric are the reinforcing yarns (i.e., the warp yarns are along the tension direction).

Reference laminated specimens were also produced for comparison in which a "clean" glass fabric (not impregnated with fillers) was placed in the cement paste; these composites will be referred to here as reference (REF). Two different fabrics were used to prepare reference composites having warp yarns of 1200 tex and warp yarns of 2400 tex. This was to study the effect of yarn tex and thickness on composite properties. Reference composites were prepared so that warp as well as weft yarns are located along the reinforcing direction, in order to examine the effects induced by fabric direction.

In all reference and filler composites, each specimen was composed of three layers of fabric, providing about 3% reinforcement by volume of yarn in the reinforcing direction. After preparing the laminated composites, a pressure of 400 N (0.004 MPa) was applied on top of the fresh composite plates for 24 h in order to improve cement penetrability between the fabric openings. The pressure was set to a level that provides a relatively constant thickness of 8 mm for the specimens.

All specimens were cured in normal wet conditions (100% RH at room temperature, 23 °C) for 13 days and then for another 21 days at room conditions (23 °C and 60% RH). Several of these specimens were additionally exposed to accelerated aging by immersing the specimens in water at 50 °C up to 21 days for all systems (including the reference), and also for 48 days for the reference system only. After the accelerated aging, the specimens were stored at room conditions for 21 days until testing. The specimens were tested for tensile behavior before and after the accelerated aging exposure, with the tests themselves performed on specimens in air-dry conditions in both cases.

The specimens will be referred here as XXYYYZZ/+weft, where XX gives the type of fabric used: 12 — warp yarns of 1200 tex or 24 — warp yarns of 2400 tex; YYY gives the filler type: SFL, SFS, SAF, PSP (see Table 1), and REF for the Reference sample with plain cement matrix (no filler); ZZ gives the accelerated aging days (in hot bath): 00 — normal un-aged curing, 21 — accelerated curing for 21 days, and 48 — accelerated curing for 48 days. Weft is added only if the reinforcing yarns of the fabric are the weft yarns; in all other cases the reinforcing yarns are the warp yarns.

2.4. Specimen testing

2.4.1. Mechanical properties

All the laminated composite systems (cement–fabric–filler) in both curing conditions – un-aged and aged – were tested in closed loop tensile test, using a Hounsfield machine with a speed of 0.5 mm/min. The test was carried out until 4% strain was gained or, if less, until complete failure of the composite. The tensile specimens were 250×30×8 mm in size (length×width×thickness). Steel plates were glued on both specimen faces, at the edges, to provide better stress transfer during testing when loaded in the grips. Five samples were tested for each system and their average properties were retrieved: first crack stress, maximum stress (UTS), energy consumption calculated by the area under the stress–strain curves, average crack spacing, and bond strength. Representative samples (with mechanical response close to the average) were graphically compared.

The crack spacing was recorded by high resolution camera, captured at 15 s intervals during loading. Using a digital processing toolbox, the images were processed to quantitatively measure the crack spacing and density as a function of the applied strain. The average crack spacing for each strain level was correlated with the stress–strain response. For more details see [12].

Table 1
Filler types and properties.

Material	Filler	Manufacturer	Description	Average particle size [nm]	T_g [°C]
SFS	Silica fume small	Cembeinder 8, Eka Chemicals AB	White silica fume	50	n/a
SFL	Silica fume large	Elkem Microsilica Grade 500 S, Elkem Materials	Purple silica fume	200	n/a
PSP	PolyStyrene particle form	Styrofan® 2D	Pure polystyrene	200	100
SAF	Styrene acrylic film-forming	Acronal® S400	Aqueous copolymer dispersion of an acrylic ester and styrene	200	−6

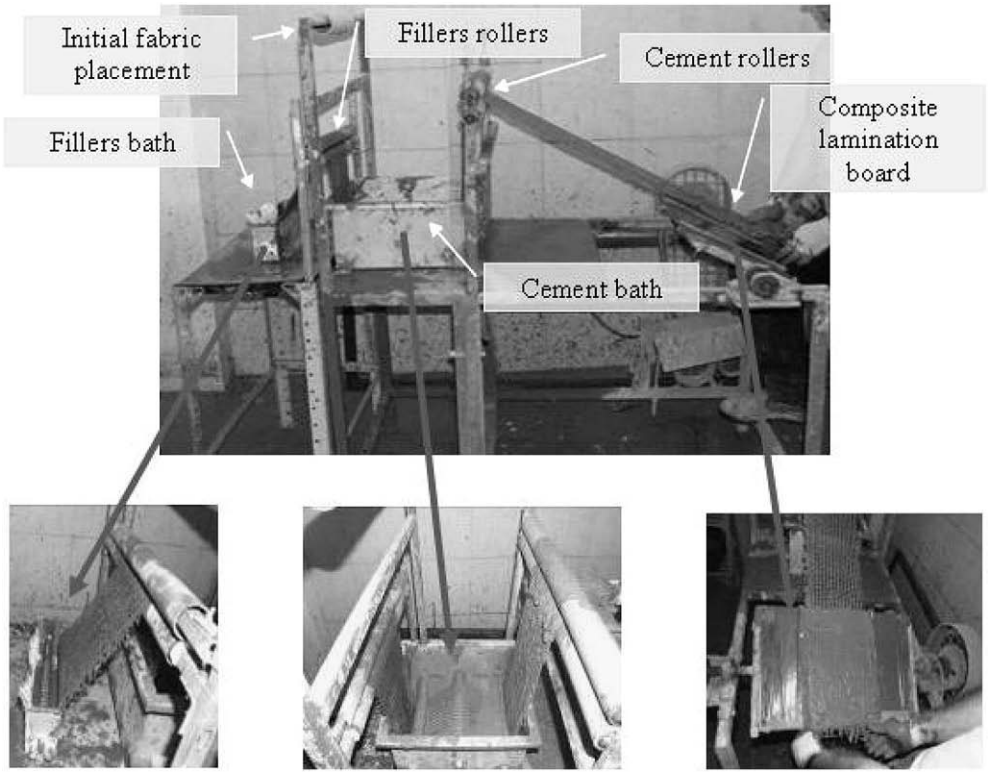

Fig. 3. The pultrusion method used for the fabrication of the composites.

2.4.2. Microstructural characteristics

In order to reach better conclusions from the mechanical test results, the samples were also characterized by Scanning Electron Microscopy (SEM) and Atomic Force Microscope (AFM). The samples for both microscopes were cut from the representative sample of each system after tensile test and polish, exposing the cross-section of the bundles embedded in the matrix. The area of cut was determined between cracks, in order to look at an area with as little damage as possible. The microscopy samples were cut to a dimension that contained three pairs of bundles (~1.5 cm) and to a thickness applicable for the microscope stages (~1 cm). For each microscopic test, 4 samples were made, and from those one was determined using optical microscope to be the representative sample for analysis. The area of interest for the SEM samples was the entire bundle and detailed analysis of the sleeve and core regions. The area of interest for the AFM samples was only the sleeve region, as it was too difficult to scan the core region due to its porous structure. In addition, for the SEM microscope another set of samples was prepared by splitting the sample along its length (along the reinforcing bundles), thus providing a different observation, top view of the entire embedded reinforcement; no polishing was applied in these cases.

3. Results and discussion

3.1. Fabric types

In order to choose the proper fabric for this research and understand its behavior and influences, two tests were performed: 1) Testing the tensile properties of the fabrics themselves, i.e., without cement (Table 2); 2) Reference composite samples (with cement but without fillers) were tested in tension before and after aging in a hot bath (Fig. 4). As mentioned, two fabrics with 1200 tex warp yarns and 2400 tex warp yarns were examined. The fabrics themselves as well as the reference composites were measured along both the warp and weft directions of the fabric. Note that the weft yarns were 1200 tex in both fabric types.

In general, similar properties, strength, and modulus of elasticity were observed for all fabrics tested along the 1200 tex yarn, whether weft or warp (Fabrics A, B, and D, Table 2). A slight reduction in fabric properties is obtained with the 1200 tex fabric tested along the warp direction (Fabric A, Table 2). In the warp direction the bundle is held tight by the stitches that form the knit structure (Fig. 2). This tightening effect can result in a wavy structure of the warp yarn, leading to less efficiency of this yarn and reduction in fabric performance through the tensile direction. When the yarns along the warp direction are thicker, as in the case of the 2400 tex, this waviness is more significant and therefore the tensile properties of the fabric (Fabric C, Table 2) are much lower in both tensile strength and modulus of elasticity, compared to other tested fabrics (tested along the 1200 tex yarn).

However, when comparing the tensile behavior of the composite reinforced with these fabrics (within the cement matrix) in the different fabric directions (warp and weft), the trend is completely different. The best tensile properties are observed for the composite

Table 2
Tensile properties of the fabrics along the warp and weft directions (no cement or fillers).

Fabric reference	Warp bundle tex	Loading direction	Yarn tex in loading direction [g/Km]	Tensile strength* [MPa]	Modulus of elasticity [GPa]	Elongation at max. stress [%]
A	1200	WARP	1200	1028 (104)	66	1.86
B	1200	WEFT	1200	1325 (113)	67	2.22
C	2400	WARP	2400	881 (87)	47	2.20
D	2400	WEFT	1200	1238 (41)	69	2.23

*Number in parentheses is the standard deviation.

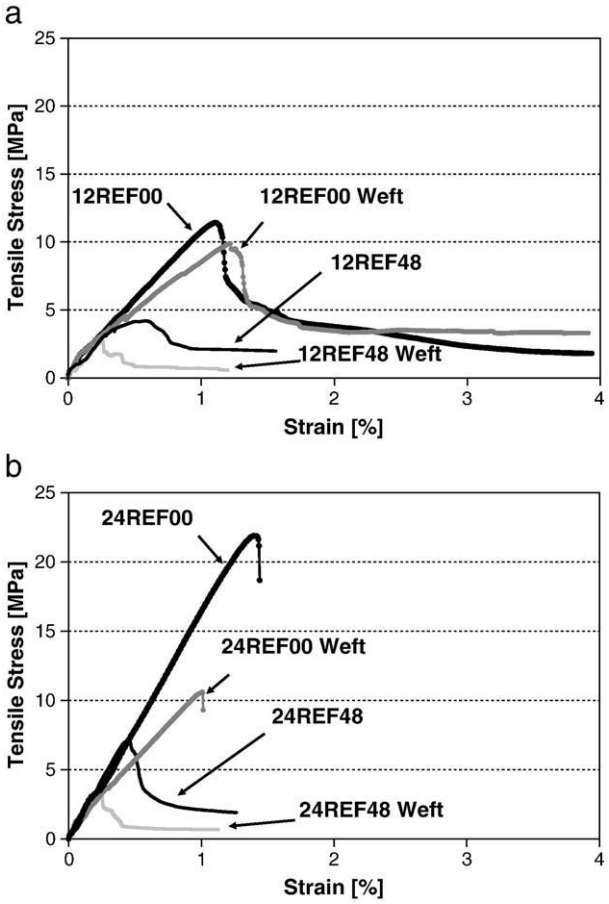

Fig. 4. Reference composites with different fabrics and test direction, at normal and accelerated curing. a) 1200 tex fabric, b) 2400 tex fabric.

reinforced with the 2400 tex fabric, tested along the warp direction (along the 2400 tex yarns; Specimen 24REF00 in Fig. 4b). This is opposed to the low properties recorded with this fabric (Fabric C, Table 2). The waviness of the tested yarns that decreases the tensile properties of the fabric itself can increase the mechanical anchoring of this fabric in the cement matrix, thus improving the composite tensile strength as clearly seen for the 24REF00 composite. These trends were also reported in a previous work for various fabric types [10]. Note also that here the composite properties are the same for all cases where the reinforcing yarns are 1200 tex, tested before aging, i.e., 12REF00, 12REF00weft in Fig. 4a and 24REF00weft in Fig. 4b.

In all cases a significant reduction in composite properties is observed after aging, whether the reinforcing yarns are 1200 tex or 2400 tex (Fig. 4a and b). The composites in all cases lost at least half their tensile strength after accelerated aging for 48 days in a hot bath (comparing the specimens of REF00 to REF48).

Based on these results, it was decided to use the 1200 tex fabric having 1200 tex yarns in both directions, weft and warp, for this research. The properties of this fabric are relatively uniform and there is no significant effect on composite and fabric performance of the stitches connecting the yarns. In general, a relatively open bundle structure can help with the penetrability of the fillers.

3.2. Filler types

In order to control the telescopic pullout mode of the AR glass strands, four different fillers were impregnated between the filaments of the bundle (Table 1) and then used to prepare the composites. The structure of the bundle filaments prior to treatment is shown in Fig. 5a, and the bundle after treatment with the fillers but before incorporation into the matrix is presented in Fig. 5b–f. Penetration of the fillers between the bundle filaments is observed for all systems, compared to the empty structure of the reference bundle (not treated). All filler systems, beside the SAF, are in a particle formation. The best and the densest filling is observed for the SFL with the larger size silica fume. This is due to its large particle size that tends to adhere and stay (interlock) between the filaments. However, particles within the filaments are also seen for the SFS (small particle silica fume) and the PSP, i.e., the polymer particles (having T_g higher than room temperature: +100 °C). In the case of the SAF, whose T_g is lower than that of room temperature (−6 °C), a film formation is observed (Fig. 5c and f). The SAF polymer sets during the drying cycle at room temperature (prior to incorporation into the cement matrix) and creates a continuous film around the filaments of the bundle, i.e., the bundle is completely coated and sealed with the polymer film.

These treated bundles were used to prepare the composites for the tension tests of normally cured and accelerated cured specimens. The results of these composites are discussed below.

3.3. Un-aged composites, normally cured

3.3.1. Mechanical performance

The tensile test results of the composites with the various fillers are presented in Fig. 6. The average values of tensile strengths, energy absorption and first crack stress (BOP) with their standard deviations are presented in Table 3.

The impregnated fillers within the glass bundle drastically change the tensile properties of the composite (Fig. 6). All the filler-treated composites showed improved strain capacity compared with the reference composite (without filler) in failure, but also at maximum stress. In all treated systems the strain values are greater when the composite reaches its ultimate stress. The most ductile behavior is observed for the SAF, the film-forming polymer; however, this composite exhibits the lowest tensile response, even below the reference. This may be indicative of the weakening effect of the film. Two of the filler systems also showed improvement in tensile strength compared to the reference composite: the SFL composite (filling with the large size silica fume) and the PSP system (filling with polymer particles not forming a film). The strength is similar for the two filler systems but the PSP exhibits more ductile behavior, which is also manifested in higher energy consumption. This might be related to the ductile polymeric properties of the PSP, and the more brittle silica fume particles with higher stiffness properties. The first crack stress (BOP) is also dependent on filler type, similar to the maximum stresses. SFL and PSP systems exhibit the highest BOP, whereas the lowest is observed for SAF. The energy absorbed during tensile loading is also highly influenced by the fillers; all the filler systems, except the SAF, exhibited enhanced energy absorption compared to reference system (Table 3).

The above trends suggest that the impregnation of the multifilament reinforcement with particulate material improves the bond with the higher modulus particles (silica fume versus PSP polymer) and therefore is more effective. The presence of the filler particles between the filaments of the bundle can lead to better transfer of the stresses from the matrix to the external filaments, but even more important, it improves stress transfer from the matrix to the inner filaments of the bundle, which are relatively far from the matrix and inaccessible when no fillers are impregnated. This inner stress transfer mechanism can enhance filament efficiency within the bundle, thus increasing the overall mechanical performance of the composite. Stiffer particles (stiffer than the glass filaments, such as the silica fumes) can transfer and carry the stresses in a more efficient manner (than ductile materials such as polymer) and therefore are more effective in multifilament-glass–cement systems.

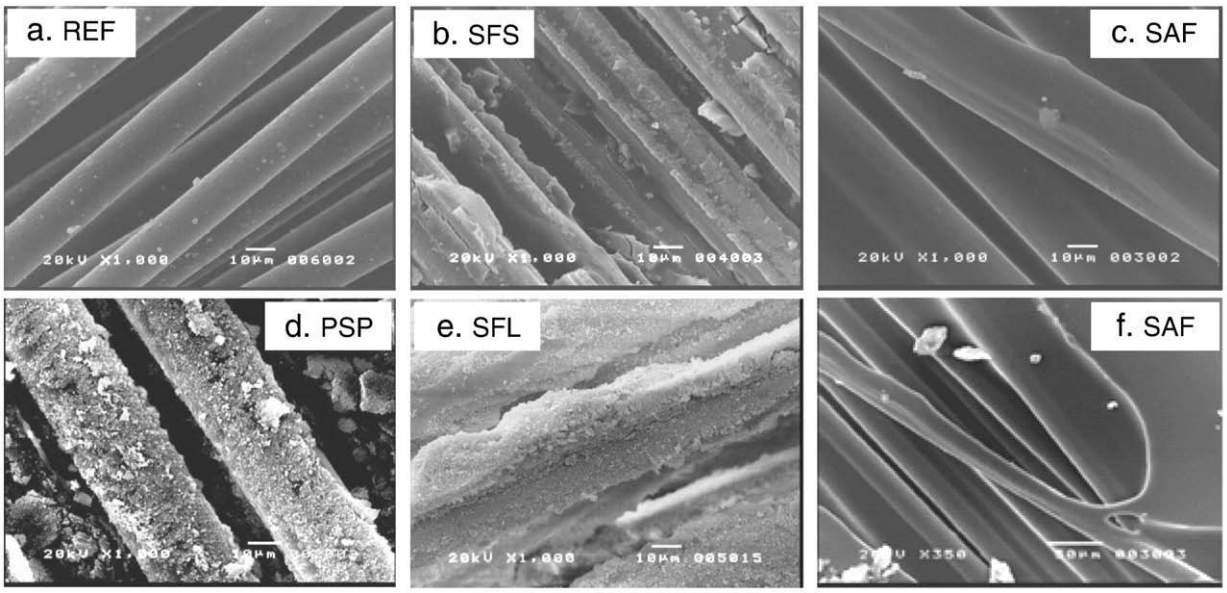

Fig. 5. Glass bundle impregnated with the different fillers prior to incorporate into the cement matrix, SAF is given in two magnifications.

3.3.2. Microstructure characteristics

The microstructure of the reference (REF) and SFL composites taken by SEM are presented in Fig. 7. These images are taken on polished specimens, viewing the cross-section of the bundle embedded in the cement matrix. The improved filling of SFL particles between the filaments of the bundle is clearly demonstrated. Many more open and empty spaces are observed for the REF system. The improved filling of the SFL is also clear when observing the zone of the core filaments compared to the REF (Fig. 7d and b, respectively). Filling is seen between the core filaments of the SFL; empty zones are observed between the core filaments in the REF. This underlines the advantage of the large silica fume particles — to fill the spaces even between the core filaments and by that improve the whole bundle efficiency. This correlates well with the improved tensile properties and bonding strengths of the SFL system (Fig. 6, Table 3). A similar trend was also seen for the PSP and SFS systems, however to a smaller extent (similar to the trends observed for the treated bundle not embedded in the matrix; Fig. 5b and d). It can be concluded that, with particulate fillers, the particles fill the empty spaces between the filaments of the bundle and thus contribute to more efficient transfer of stresses even to the bundle core, providing better tensile properties and bonding compared to the REF system, mainly for the SFL and PSP.

In the case of the SFS only (the small silica fume particles), intense micro-cracking at the interface zone of the sleeve filaments–matrix is observed (Fig. 8a). When looking at the sleeve filament with higher magnification, a dense layer of silica fume particles covers the filament (Fig. 8b), indicating good bonding. These observations can explain the mechanical properties and behavior of the SFS system: high bonding on one hand, but its relatively decreased tensile strength due to the development and presence of micro-cracks at the interface zone. These micro-cracks can be due to the very fine particle size (50 nm) of the silica fume, leading to a dense but brittle matrix at the interface.

The SAF system, a film-forming polymer with low T_g, impregnated in the cement matrix is presented in Fig. 9. Also, within the matrix the formation of the film around all filaments of the bundle is clear. The film coats the filaments and the bundle completely. The ductile properties of this film can result in malleable behavior under tension in this system (Fig. 6), however, this film probably creates a barrier having poor adhesive properties with the matrix, leading to the poor tensile strength of this system.

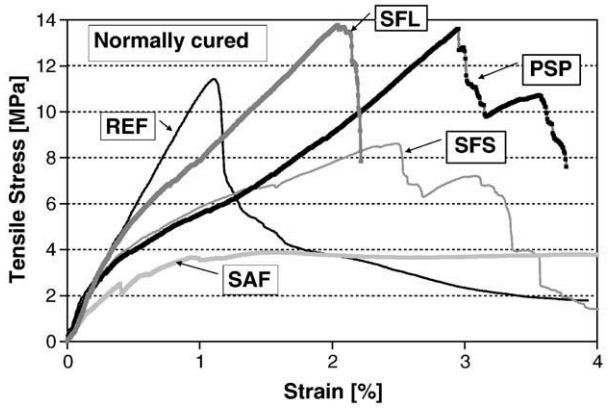

Fig. 6. Tensile behavior of un-aged composites.

3.4. Accelerated aged composites

One important objective of treating the bundle with fillers is to improve the service life of the composite. Accelerated aging was performed to evaluate the composites' durability and the influence of the fillers on the composites over time.

As mentioned, during continued hydration and aging a gradual process of deposition of hydration products between the filaments takes place, which may change the nature of bonding by increasing the sleeve/core ratio, and can result in embrittlement of the composite.

Table 3
Average results of the un-aged, normally cured composites.

	SFS	PSP	SFL	SAF	REF
Tensile strength [MPa]	8.78 (1.02)	13.61 (1.60)	14.61 (1.92)	3.77 (0.36)	11.22 (1.93)
Energy up to max strength [J/cm^3]	0.150 (0.008)	0.205 (0.045)	0.178 (0.048)	0.054 (0.010)	0.078 (0.017)
BOP strength [MPa]	2.11 (0.79)	3.67 (0.70)	2.28 (0.27)	1.70 (0.56)	2.06 (0.32)
BOP strain [%]	0.204 (0.090)	0.462 (0.150)	0.149 (0.020)	0.259 (0.116)	0.134 (0.021)

Number in parentheses is the standard deviation.

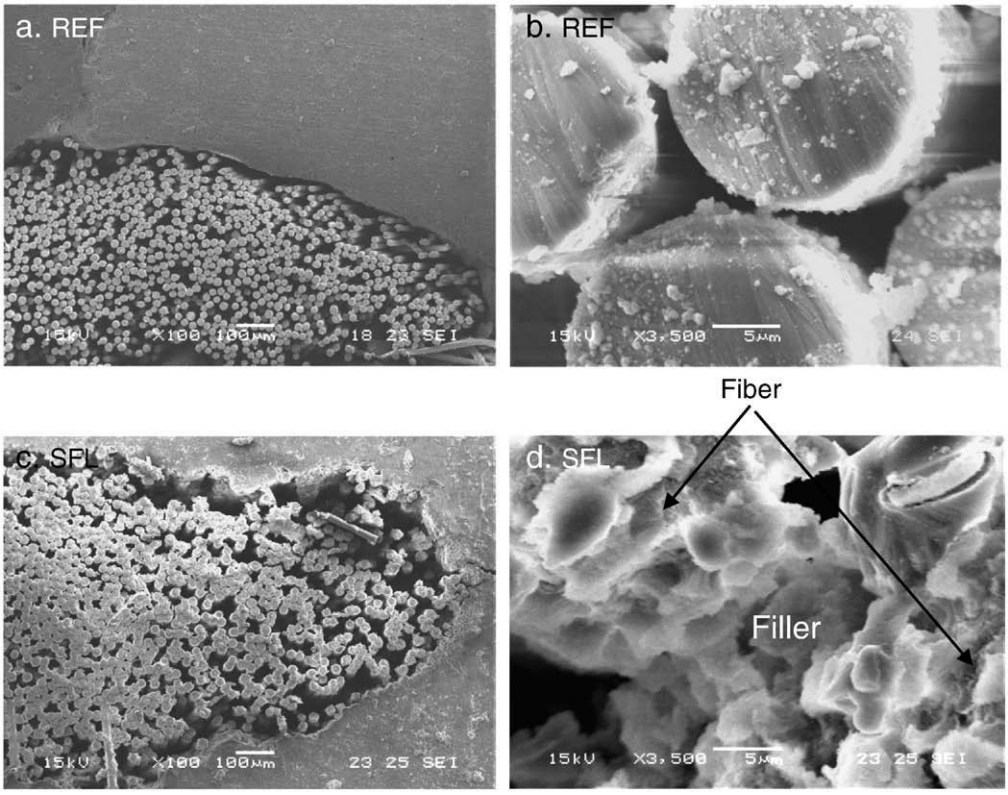

Fig. 7. Glass bundle embedded in the matrix. Observations on the cross-section of the embedded bundles: (a) REF × 100; (b) REF at the bundle core, × 3500; (c) with SFL filler (large silica fume) × 100; (d) SFL at bundle core, × 3500.

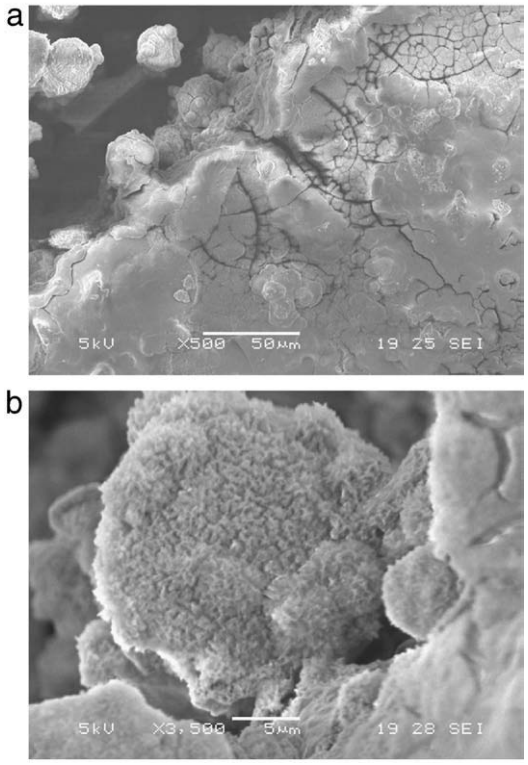

Fig. 8. SEM images of SFS filler composite at the sleeve filaments. (a) External filament at × 500 magnification, (b) closer observation on the external filament at the ITZ, × 3500 magnification.

3.4.1. Mechanical performance

For choosing the optimal aging period for this research, REF samples were tested in tension at different accelerated curing durations: 1, 3, 7, 14, 21, and 48 days in a hot bath (50 °C). These results are presented in Fig. 10, showing the relation between the tensile strength of the composite and the duration of aging. From those results it is seen that the tensile strengths of the composite are reduced over time up to 21 days, after which no further reduction is observed. The reduction in tensile strength was 60%. Also, reductions in energy consumption of about 85% was recorded during that time. Based on that, the duration for accelerated curing was fixed as 21 days in a hot water bath for all filler systems.

The tensile behavior and properties of the different systems after accelerated aging are presented in Fig. 11a and Table 4. The tensile performance, strength, and energy of the different filler systems before and after accelerated aging are presented in Fig. 11b (energy is shown as bars and tensile strengths as dots). The change in percentage of the tensile properties due to aging (ratios between

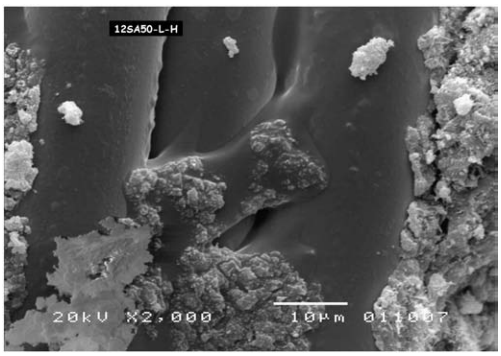

Fig. 9. Glass bundle impregnated with SAF polymer, forming a film, after incorporation into the cement matrix.

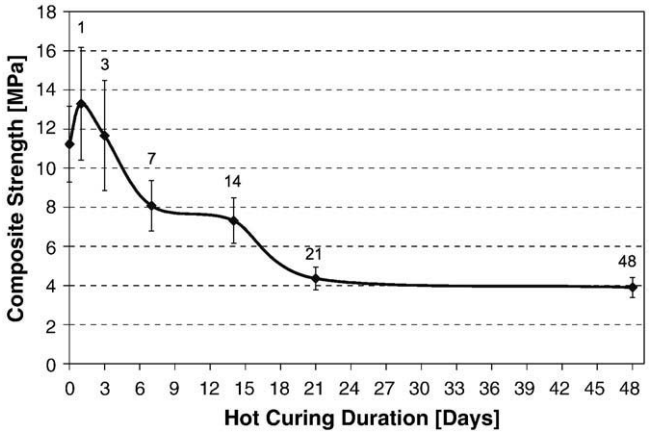

Fig. 10. Tensile strength of REF composites accelerated cured for different periods.

composite properties before and after aging of each system) is shown in Table 5. The tensile responses before and after accelerated curing are presented in Fig. 12, along with the spacing between the cracks developed during loading, for several chosen systems.

The drastic reduction in composite tensile performance of the REF system is seen again in Figs. 11b and 12a. At low strains no significant difference in tensile behavior is observed between the aged and un-aged REF composites; also crack development is relatively the same. However, at high strains the influence of aging is obvious. Brittle behavior and significant low tensile strength are observed for the REF composites after aging compared to their properties prior to aging. The spacing between the cracks is larger for the aged REF system at relatively high strain levels. The crack saturation, i.e., where no new cracks are formed and the cracks are mainly widening, occurred at a later loading stage for the un-aged system (larger strain, of about 1%). The saturation of crack formation takes place at a lower strain, of about 0.5%, for the aged system. This demonstrates that at normal curing, the bond strength is relatively high, as the multiple cracking takes place up to a relatively large strain, i.e., the bond strength is reduced due to aging.

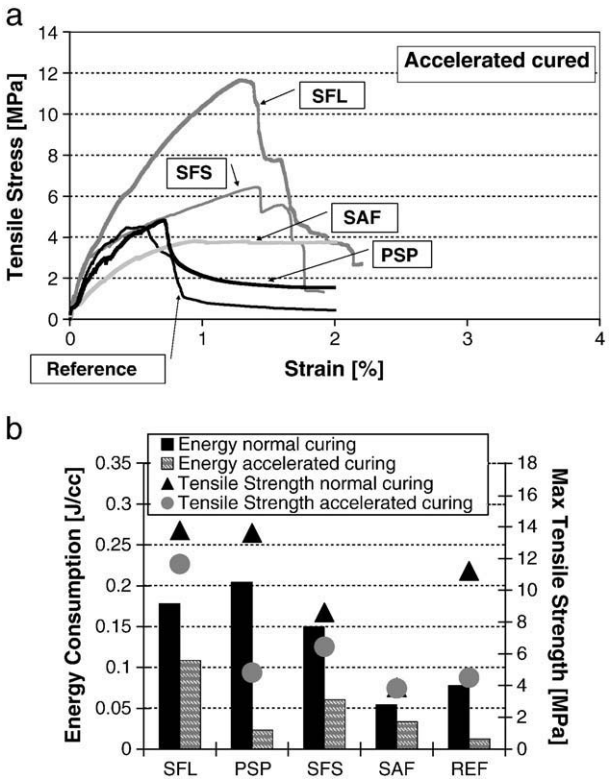

Fig. 11. Effect of aging on tensile properties. (a) Tensile response of all tested systems after aging. (b) Strength and energy consumption of the different composites, before and after accelerated aging.

Table 4
Average tensile results of the composites after accelerated curing.

	SFS	PSP	SFL	SAF	REF
Tensile strength [MPa]	5.83 (1.43)	4.98 (0.24)	10.68 (1.96)	3.66 (0.40)	4.36 (0.58)
Energy up to max strength [J/cm^3]	0.060 (0.027)	0.023 (0.002)	0.108 (0.043)	0.033 (0.012)	0.013 (0.003)
BOP strength [MPa]	1.910 (0.566)	1.693 (0.204)	2.026 (0.171)	0.345 (0.136)	0.342 (0.132)
BOP strain [%]	0.081 (0.021)	0.103 (0.024)	0.095 (0.029)	0.023 (0.009)	0.006 (0.004)

Numbers in parentheses is the standard deviation.

When comparing the behavior of all treated composites after aging, it can be seen that the fillers strongly influence the durability of these composites. More brittle behavior is observed after aging (Fig. 11a) compared to the response prior to aging (Fig. 6a), for all filler systems. Also, reduction in energy absorption is observed for all aged composites (Fig. 11b). The most drastic reduction in composite properties after accelerated aging was observed for the PSP systems (Fig. 12b) — more than 60% in strength and 90% in energy consumption (Table 5). The reduction is even greater than that obtained with the aged REF composite. The sensitivity of the PSP system to aging is the extent to which its properties after aging are similar to those of the aged REF (Fig. 11a); this is opposed to the high properties obtained with this polymer system at normal cured condition (Fig. 6). With the PSP, the spacing between the developed cracks, during tensile tests, is larger after aging, similar to the REF composite. This indicates again that the bond is reduced over aging with this polymer filler system. The crack widening process starts at a very early stage, at a low strain of about 0.75% for the aged composite system. In the case of the un-aged PSP composite the multiple cracking continues through almost the entire testing. This suggests better stress transfer before aging, which drastically reduced over time. The SFS also showed reduction in tensile properties after aging but to a lesser extent.

The best performance was obtained with the SFL-treated composite, indicating the favorable effect of the larger silica fume particles (Fig. 11a). The SFL composite exhibits only mild reduction in composite properties, tensile strength, and energy consumption after accelerated aging (Fig. 11b). The composite after aging is more brittle and stiffer (Fig. 12c). The spacing between the developed cracks of the SFL system is slightly larger for the un-aged composite compared with the aged composite, mainly at low strains, suggesting that the bond is even improved to some extent during aging. However, with large strains there are no significant differences between the crack spacing of the aged and un-aged SFL specimens, meaning also that no drastic change in bond strength occurred during aging with the large silica fume system. More importantly, the properties of the SFL composite after aging are similar to and even better than those of the un-aged REF (Fig. 11b). This demonstrates the advantage of the larger silica

Table 5
Percent change in composite tensile properties before and after aging*.

[%] Sys.	Tensile strength	Energy
REF	−61	−84
PSP	−65	−89
SAF	−2	−38
SFL	−15	−39
SFS	−25	−60

*Calculated as: 100 (accelerated curing property − normal curing property)/normal curing property.

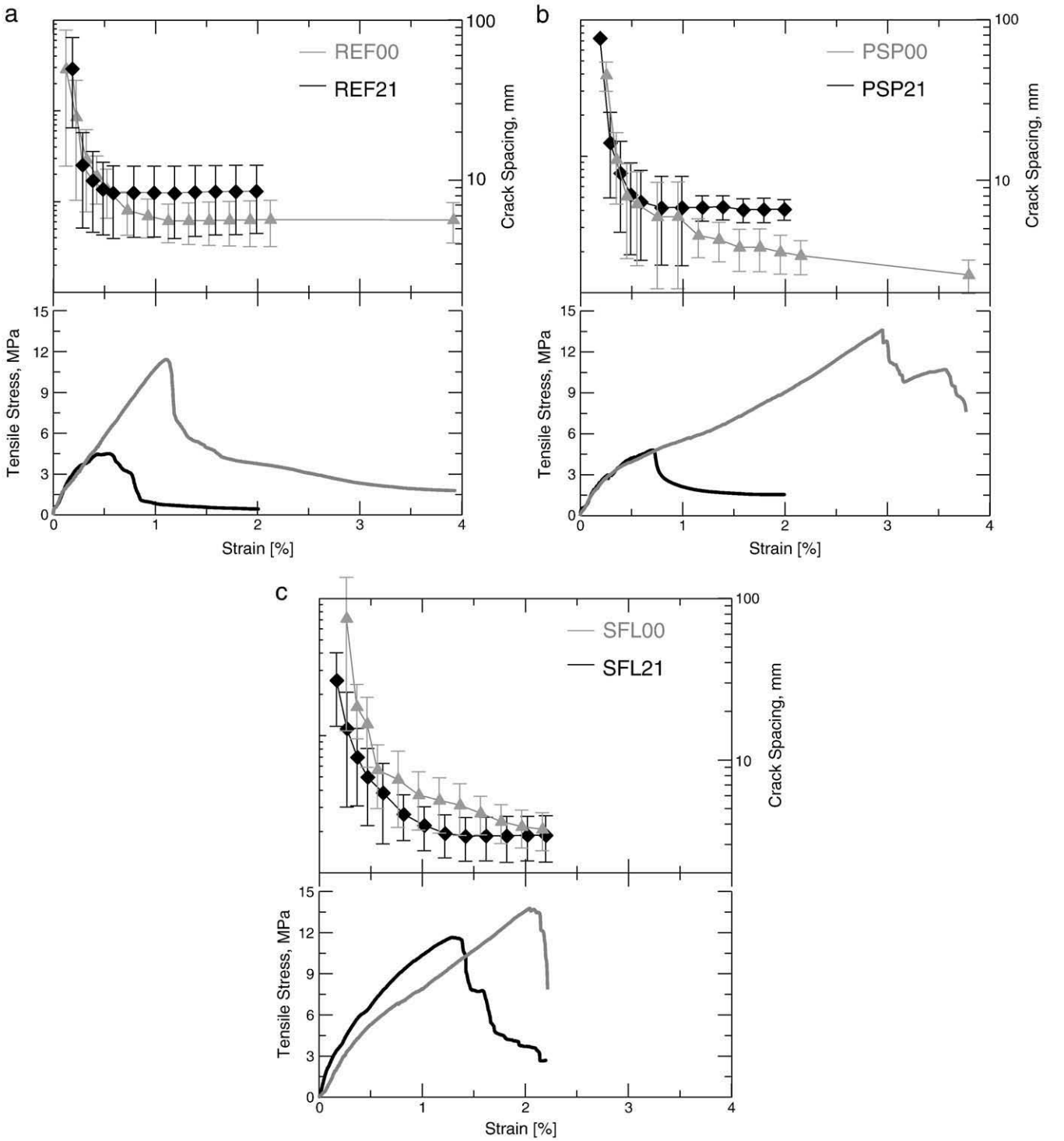

Fig. 12. Tensile response and cracking spacing of composites exposed to normal curing (00) and accelerated curing (21). (a) REF system, (b) PSP system, (c) SFL system.

fume particles, which makes it a superior reinforcing system. It should be noted that the film-forming treatment, SAF, showed a favorable retention of properties during aging, but its initial properties (at normally cured conditions) were not as good as the other treated and reference systems, so this treated system does not have a real benefit for GFRC.

3.4.2. Microstructural characteristics

SEM observations on the REF composite (without fillers) before and after accelerated aging are presented in Fig. 13. These images clearly show that during continued hydration and aging a process of deposition of hydration products takes place between the filaments. The spaces between the filaments of the bundle prior to aging are relatively empty (Fig. 13a and b), as no fillers were used to fill these spaces. However, after aging, these areas between the filaments are no longer as open, and a thick layer of cement products around the core filament is observed (Fig. 13c and d). This can change the nature of bonding by increasing the sleeve/core ratio and leading to improved bond strength, as it increases the number of fibers that are in direct contact with the matrix. Greater bond strength is expected to enhance composite tensile strength but lead to embrittlement. The significant increase in brittleness of the composite with aging was clearly seen in

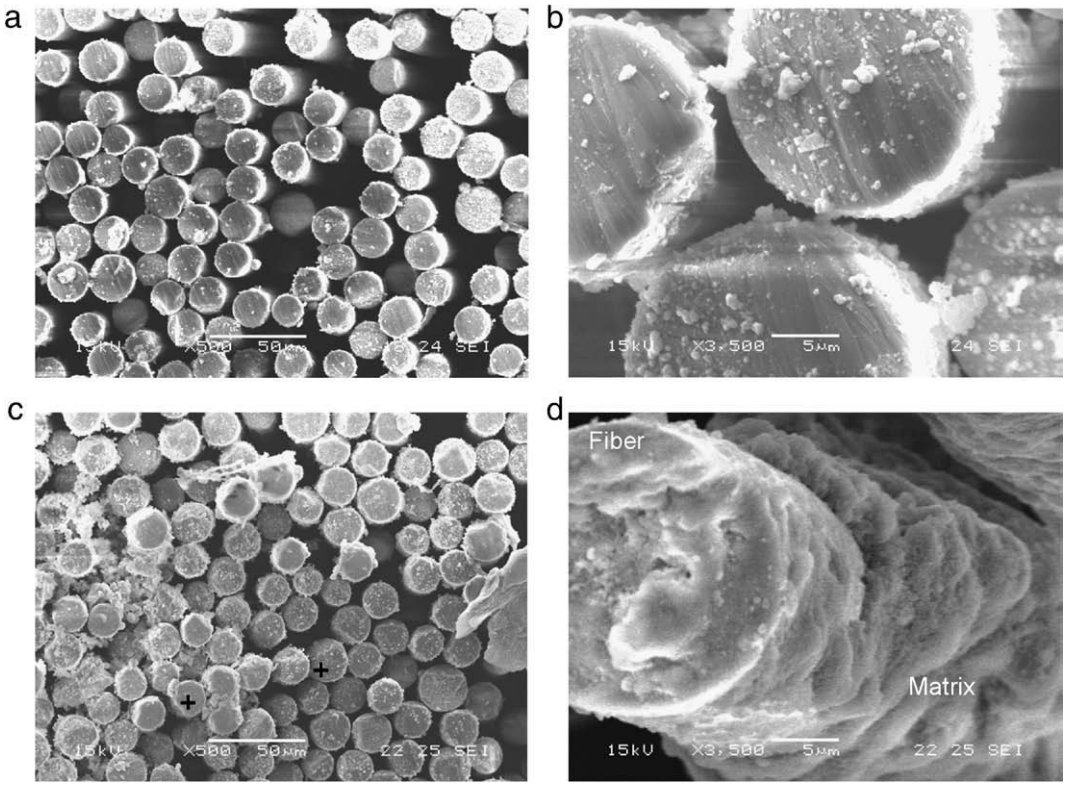

Fig. 13. REF composites, core filaments: (a, b) un-aged, normally cured; (c, d) aged specimens in hot bath.

Fig. 12a. However, a drastic reduction in composite strength was also observed after aging.

When observing the interfacial zone between the fibers and the matrix of aged and un-aged REF composites, a difference in the microstructure of the hydration products is seen in each aged system. In the case of the un-aged composite, the cement hydrates are in relatively small units and compacted together, resulting in a quite dense cement layer around the perimeter of the bundle (Fig. 14a), as mentioned not many of such products were penetrated in between the filaments bundle. In the case of the accelerated aged composite two main hydrate products are observed: (i) relatively large products that are not well compacted around the fiber perimeter, leaving many empty pores between them (Fig. 14b); and (ii) tiny needle structure hydrates that are dispersed between the large products (Fig. 14c). This microstructure provides a relatively porous layer around the filament, which might be related to corrosion of the cement paste over time. The increased porosity around the filaments after aging was also observed under the AFM (Fig. 15). Large pores are seen after aging (Fig. 15b), whereas a relatively dense matrix is observed prior to aging (Fig. 15a). This porous structure may lead, at least to some extent, to the reduction in its tensile strength. In addition, due to the increased penetration of the cement products into the filaments during aging (Fig. 13), more fibers are directly touching the matrix in the aged REF system. It is well known that glass fibers are sensitive to the alkali environment of the cement matrix, and suffer from etching (corrosion) when they are in intimate contact with cement products. Such corrosion mechanisms of the glass fibers may apply also here, leading to reduction in fiber tensile properties and the overall behavior of the composite after the accelerated aging. Note that the glass fibers used in this work were an alkali resistant type but no coating with sizing was employed. When observing Fig. 13c carefully, some irregularity in filament cross-section shape is observed in the case of the aged composite bundle, for a few filaments only (two are labeled with + in the figure), which may imply such an alkali attack. Note that in the case of the un-aged bundle all filaments are in full round shape (Fig. 13a).

In a similar trend as above, penetration of hydration products between the filaments of the bundle during aging is observed for the

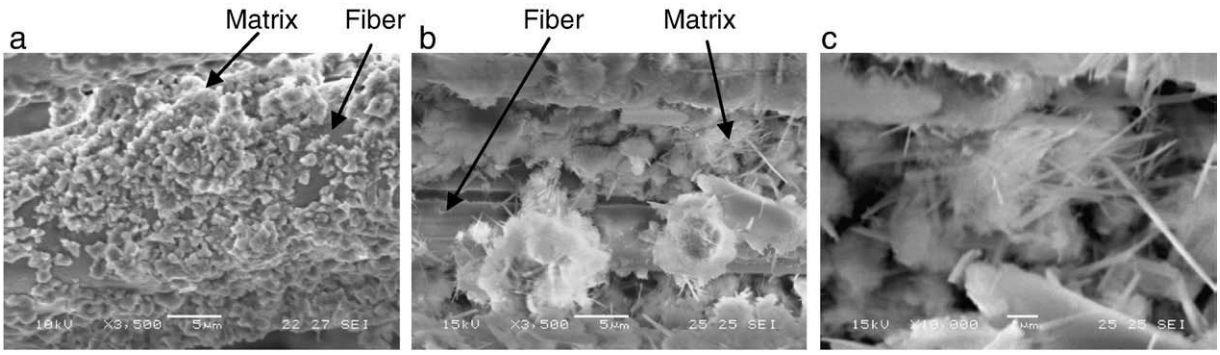

Fig. 14. Structure at the filament inside the matrix of REF specimens: (a) un-aged after normal curing (×3500); (b, c) after accelerated aging (×3500 and ×10,000, respectively).

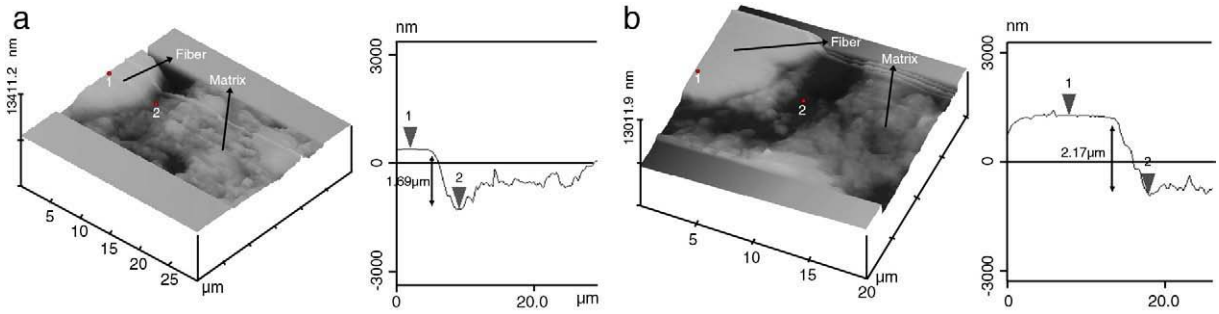

Fig. 15. REF, sleeve. ITZ formation between sleeve fiber and the matrix obtained by AFM: (a) after normal curing, (b) after accelerated curing.

PSP system (Fig. 16). Here, in the case of the PSP, the deposition process of cement hydrates into the bundle during aging is even more aggressive than that observed for the REF system. The polymer particles are clearly seen between the core filaments of the bundle before aging (Fig. 16a), but after the accelerated aging massive and very dense products are observed between those filaments of the bundle (Fig. 16b). This means that the polymer particles of this filler cannot prevent the transition of cement products into the bundle during aging, although they can highly improve the stress transfer within the bundle, providing high performance at an early age (Fig. 12b). In this polymer system (PSP) the chemical attack and the corrosion process of the individual filaments within the bundle during accelerated curing is more obvious than in the case of the REF. After aging, most of the fibers do not keep their original round shape and some parts are missing, as clearly shown in Fig. 16b. This can happen when the filaments directly touch the alkali cement products. These mechanisms can lead to the extremely high reduction in composite tensile performance obtained with the PSP system after aging in strength, toughness, and ductility (Fig. 12b).

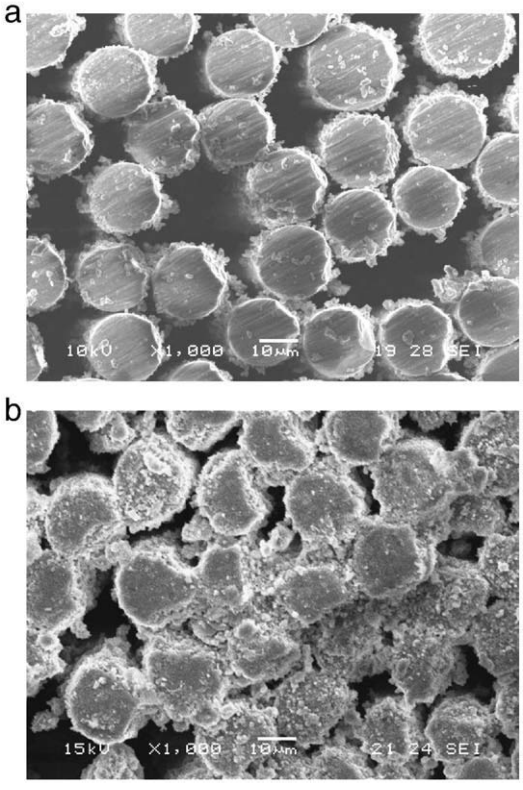

Fig. 16. Core, SEM images of the core filaments imbedded in the cement matrix of (a) PSP system normally cured, (b) PSP system after accelerated curing.

The situation is quite different for the SFL composite; in this large silica fume particle system no significant difference in microstructure was observed before and after aging. In both cases similar silica fume particles were seen between the core filaments (Fig. 7c and d). This means that the silica fume particles can limit the deposition of the cement products between the bundle filaments over time, keeping the properties of the composite even after in late stages (Fig. 12c). The SFL system showed extremely high resistance to the accelerated curing; after aging strength and energy were larger than the un-aged REF system (Fig. 11b). Due to the stiffness and large particle size of this filler, it may better interlock within the bundle and not be easily pushed away by active cement products, thus providing improved durability for GFRC components.

Note that for the SFS, small silica fume particle filler, some deposition of cement products was observed but not as much as in the case of the REF and PSP, leading to reduction in composite performance over time but not as significantly. These observations correlate with the magnitude of reduction in tensile results over time of this composite (Fig. 11b). In this case of the silica fume, maybe the small size particles (SFS) could not interlock within the bundle filaments as well as the large particles (SFL), and therefore could not maintain the hydrate deposition over time as well.

Film around the bundle filaments was also observed after aging for the SAF system, similar to the un-aged composite (Fig. 9). This film protects the fibers from corrosion and prevents penetration of the cement products between the filaments during aging; therefore, it showed a favorable retention of properties over time (Fig. 11). However, its initial properties (at normally cured conditions) were relatively low compared to the other treated and reference systems (Fig. 6), so its high resistance to aging is quite limited.

4. Conclusions

- Composite properties can be controlled by addition of fillers into the fabric yarns; the magnitude and efficiency of the modification is highly dependant on the type, structure, and properties of the filler.
- Fillers that have a particle nature are likely to improve the composite properties better than fillers that have a film formation nature, as the particulate fillers can retain the effects induced by the telescopic pullout mode and at the same time transfer the stresses from the matrix to the inner filaments, improving the overall efficiency of the bundle. The particle size should be large enough, as colloidal particles of several tens of nanometers can cause micro-cracks in the matrix that eventually damage the tensile strength of the composite, although the bond strength may be improved.

- Two main degradation mechanisms were observed during aging, both due to matrix penetrability into the bundle: (i) changing the telescopic pullout derived by cement penetrability, as more fibers fracture after aging, leading to more brittle behavior; and (ii) chemical deterioration of the glass fibers themselves as more fibers are in direct contact with the cement matrix, reducing composite strength. Therefore, favored filler systems are those that moderate cement hydrates' penetrability between the bundle filaments over time, keeping the telescopic pullout mode and composite ductility, and at the same time protecting the core filaments from chemical attack, thus retaining their high performance and the overall tensile strength of the composite.
- The best performance with respect to initial properties and the retention of strength and energy after aging was obtained with the SFL system. The other two particulate systems, SFS and PSP, did not perform as well. Favorable retention of properties upon aging was also obtained by the film-forming SAF system, but the initial properties were lower.
- The particulate effect requires that the particles are sufficiently small to be incorporated between the filaments in the strand and be able to maintain their particulate nature after aging, to prevent any cementing action within the strand. The fact that superior durability behavior was obtained with the larger silica fume particles (compared to the polymer particles) may suggest that two effects should be considered: (i) the need for a high modulus filler (perhaps to be effective in providing the inner "rolling" effect, the filler should not be softer than the glass filaments), (ii) eliminate reaction between the filler and the matrix (the larger silica fume particles are less prone to be engaged in pozzolanic reaction when in contact with the pore solution penetrating in between the filaments).
- When the particulate system is of a film-forming nature, the filaments in the strand are probably engulfed and protected, and thus aging is being moderated or even prevented. However, apparently the bond with the matrix is being reduced to start with, but is largely preserved upon aging. Obviously, the soft nature of the film has an impact on these characteristics, probably lowering the effective bond, but preserving it upon aging.

Acknowledgements

The authors would like to acknowledge the Israel Science Foundation grant no. 898/06 for the financial support in this research, and ITA RWTH (Aachen) Germany for providing the glass fabrics used in this research. Thanks are expressed to Elkem Materials in Norway and Eka Chemicals AB in Sweden for supplying the microsilica and amorphous silica slurries.

References

[1] W. Brameshuber, Textile Reinforced Concrete: State of the Art Report of RILEM Committee 201-TRC, RILEM Publications, Bagneux, France, 2006.
[2] A. Peled, A. Bentur, Fabric structure and its reinforcing efficiency in textile reinforced cement composites, Composites: Part A 34 (2003) 107–118.
[3] A. Peled, B. Mobasher, Pultruded fabric–cement composites, ACI Mater. J. 102 (2005) 15–23.
[4] W. Brameshuber, T. Brockmann, B. Banholzer, Material and bonding characteristics for dimensioning and modeling of textile reinforced concrete (TRC) elements, Mater. Struct. 39 (2006) 749–763.
[5] A.E. Naaman, Strain hardening and deflection hardening fiber reinforced cement composites, in: A.E. Naaman, H.W. Reinhardt (Eds.), Fourth International Workshop on High Performance Fiber Reinforced Cement Composites (HPFRCC 4), RILEM Publications, Bagneux, France, 2003, pp. 95–113.
[6] A. Bentur, S. Mindess, Fibre Reinforced Cementitious Composites, Spoon Press, London, New York, 2002.
[7] B. Banholzer, Bond behavior of a multifilament yarn embedded in a cementious matrix, PhD diss., RWTH Aachen, Germany, 2004.
[8] W. Zhu, P. Bartos, Assessment of interfacial microstructure and bond properties in aged GRC using novel microindentation method, Cem. Concr. Res. 27 (11) (1997) 1701–1711.
[9] A. Bentur, S. Diamond, Aging and microstructure of glass fiber cement composites reinforced with different types of glass fibers, Durability Build. Mater. 4 (1987) 201–226.
[10] M. Raupach, J. Orlowsky, E. De Bolster, P. Van Itterbeeck, J. Wastiels, H. Cuypers, Durability of glass fibre reinforced composites experimental methods and results, Compos. Part A Appl. Sci. Manuf. 37 (2006) 207–215.
[11] B. Mobasher, A. Peled, Tensile behavior of fabric cement-based composites: pultruded and cast, ASCE, J. Mater. Civil Eng. 19 (4) (2007) 340–348.
[12] J. Aveston, G.A. Cooper, A. Kelly, Single and multiple fracture, The properties of fibre composites, Proc. Conf. National Physical Laboratories, IPC Science and Technology Press Ltd, Guildford, UK, 1971, pp. 15–24.